Acta Med. Okayama, 2017
Vol. 71, No. 2, pp. 105-112

Acta Medica Okayama
http://escholarship.lib.okayama-u.ac.jp/amo/

Original Article

Diagnostic Value of Dual-time-point F-18 FDG PET/CT and Chest CT for the Prediction of Thymic Epithelial Neoplasms

Takayoshi Shinya[a]*, Takashi Tanaka[a], Junichi Soh[b], Toshi Matsushita[a], Shuhei Sato[a], Shinichi Toyooka[b], Tadashi Yoshino[c], Shinichiro Miyoshi[b], and Susumu Kanazawa[a]

Departments of [a]Radiology, [b]General Thoracic Surgery, [c]Pathology, Okayama University Hospital, Okayama 700-8558, Japan

We retrospectively assessed the dual-time-point (DTP) F-18 FDG PET/CT findings of thymic epithelial neoplasms (TENs) and investigated the diagnostic capacity of PET/CT compared to that of CT for predicting carcinoma. We calculated the ratio of the standardized uptake value of the tumor and that of the aortic arch (T/M ratio) for both the 90-min early scan and the 2-h delayed scan in 56 TEN patients. We used a multivariate logistic regression (MLR) analysis to estimate the CT features of carcinoma. We compared the diagnostic capacities of PET/CT and chest CT using receiver operating characteristic (ROC) analyses. The ROC curve revealed that the appropriate cut-off T/M ratio value for the highest accuracy was 2.39 with 75.0% accuracy. The area under the curve (AUC) was 0.855. The statistical analyses for DTP scans of 35 TEN patients demonstrated 74.3% accuracy and 0.838 AUC for the early scan versus 82.9% and 0.825 for the delayed scan. The MLR analysis indicated that mediastinal fat infiltration was a predictor of carcinoma. The ROC curve obtained for the model yielded an AUC of 0.853. Delayed scanning could improve the diagnostic capacity for carcinoma. The T/M ratio and mediastinal fat infiltration are predictive of carcinoma with moderate diagnostic accuracy.

Key words: thymic epithelial neoplasm, thymic carcinoma, thymoma, dual-time-point PET/CT, chest CT

The World Health Organization (WHO) histological classification system for thymic epithelial neoplasm (TEN) was proposed in 1999 and updated in 2004 [1] and has been widely adopted for independent prognostic factors [2,3]. The overall survival rates of patients with type A, AB, or B1 TEN are higher than those of patients with type B2 or B3 TEN [4]. Moreover, a meta-analysis clearly showed that thymomas can be distinguished in different prognostic subgroups because carcinomas are neoplasms with a more aggressive malignant potential [5].

Preoperatively, TENs are diagnosed by morphologic examinations such as computed tomography (CT) and magnetic resonance imaging (MRI). However, there are some overlapping features in the histological subtypes of TEN according to the WHO classification [6]. An earlier study of 33 TEN cases demonstrated that mediastinal fat invasion was an indicator for differentiating 3 risk groups and had a prediction rate of approx. 76% using discriminant analyses [7].

To evaluate TENs, 18-fluorine fluorodeoxyglucose (F-18 FDG) positron emission tomography/computed tomography (PET/CT) has been proposed as an advanced noninvasive imaging method. The correlation between FDG uptake and the WHO classification has been investigated [7-13], and several of these studies examined the diagnostic capacity of single-time-point (STP) PET/CT for the determination of carcinoma in 28 to 46 TEN patients [9,11-13]. In those

Received June 2, 2016; accepted September 27, 2016.
*Corresponding author. Phone: +81-86-235-7313; Fax: +81-86-235-7316
E-mail: midnight-2005@nifty.com (T. Shinya)

Conflict of Interest Disclosures: No potential conflict of interest relevant to this article was reported.

analyses, PET images were analyzed with qualitative or semiquantitative methods, such as the calculation of the maximum standardized uptake value (SUVmax) or the tumor-to-mediastinum (T/M) ratio. Several recent studies have shown the usefulness of dual-time-point (DTP) PET for evaluating the malignant nature [14-16]. For the TEN patients, only one study has reported the performance of DTP PET/CT using 60-min and 3-h scans after tracer injection with no evaluation of the diagnostic accuracy of the delayed-scan for carcinoma [11].

The aim of the present study was to retrospectively assess the DTP PET/CT findings of TEN cases using a simplified WHO classification scheme that employs 3 risk groups: type A, AB, and B1 = low-risk thymoma (LR); B2 and B3 = high-risk thymoma (HR); and thymic carcinoma (CA). We also investigated the diagnostic capacity of PET/CT for differentiating thymic carcinoma from thymoma and compared it to the diagnostic capacity of chest CT.

Materials and Methods

Patients. The study was a retrospective analysis of data collected between August 2006 and September 2014 at Okayama University Hospital. A total of 56 patients were included (32 men, 24 women; age [mean ± SD] 60.63 ± 14.98; range 21-86 years). The inclusion criteria were as follows. Each patient had: a minimum patient age of 20 years; a definitive diagnosis of TEN; a chest CT at our institution and an F-18 FDG PET/CT at an adjacent imaging center before biopsy or surgery; no therapy before the PET/CT and CT examination. We classified the TENs using the WHO criteria. Each TEN was also graded into one of the above-described 3 risk groups by pathologists who were unaware of the PET results. All tumors were staged according to the Masaoka clinical-pathologic staging system [17].

This study was approved by the ethical committee of our institution (approval no. 2244), and the requirement for the patients' informed consent was waived.

F-18 FDG PET/CT and image data analysis. For the F-18 FDG PET/CT, the patient fasted for at least 5 h, after which blood glucose levels were determined to ensure a level of < 140 mg/dL. The patient then received an intravenous injection of 3.7 MBq/kg of body weight (1.0×10^{-4} Ci/kg) of F-18 FDG. With the patient in a relaxed supine position, the PET/CT image acquisition started at 90 min (early phase) and at 2 h (delayed phase) after the FDG injection, using an integrated PET/CT scanner (Biograph LS/Sensation 16, Siemens, Munchen, Germany). First, a total-body low-dose CT scan for the calculation of attenuation correction was performed. It used a standardized protocol involving 140 kV, 12 to 14 mAs, a tube-rotation time of 0.5 sec per rotation, a pitch of 0.8, a section thickness of 3 mm, and a scan field from head up to the mid-thigh level.

Subsequently, PET images consisting of 7-8 bed positions with 2.4 min per table position over the same region were obtained using a three-dimensional high-sensitivity mode with an axial field of view of 70-cm in a 168 × 168 matrix. A 46-mm overlap was used between the bed positions. The PET images were reconstructed iteratively on a 168 × 168 matrix using an ordered-subset expectation maximization (OSEM) algorithm for 8 subsets and 2 iterations, with a 5.0-mm post-reconstruction filter. In-plane resolution of 4.2-mm and axial resolution of 2.0-mm were obtained. The PET images were reconstructed with an OSEM iterative reconstruction algorithm.

Two nuclear physicians unaware of the histological results interpreted all PET/CT findings by consensus. First, the SUVmax was adopted for the semiquantitative evaluation of FDG uptake. It was calculated using the following formula: SUVmax = maximum tissue concentration (MBq/g)/injected radioactivity (Bq) per body weight (g). The SUVmax calculation required manually setting the volume of interest (VOI). The T/M ratio, which is the ratio of the tumor SUVmax to the background mediastinum SUVmax, was then determined for each patient. The aortic arch was taken as the reference region for mediastinal activity.

For a semiquantitative analysis of FDG uptakes, we used the T/M ratio in order to avoid the bias derived from the use of SUVmax, which could be altered by several technical factors [18, 19]. The T/M ratio measurements were obtained for both the early scan (T/M ratio1) and the delayed scan (T/M ratio 2). VOIs were drawn to encompass the TEN contours on PET/CT images.

Chest CT and image analysis. Because the study design was retrospective, a variety of multidetector CT scanners had been used. At our institution, CT images were obtained with breath holding and the following parameters: 120 kVp, 300 mA of auto mA mode, and

a section thickness interval of 5 mm depending on the protocol used. In almost all of the patients (n = 53), intravenous nonionic contrast medium had been administered via an antecubital vein at a rate of 2.0-3.0 ml/s with a 30- to 50-sec delay. All image data were displayed as mediastinal window images (level, 30 HU; width, 350 HU).

The CT scans were reviewed by two radiologists, and differences in their findings were resolved by consensus. The CT scan findings were assessed in terms of the tumor size, the contour of the tumor, the presence of pleural effusion, and other tumor features (*i.e.*, homogeneousness, the presence of calcification, mediastinal fat infiltration, great vessel invasion, and lymph node adenopathy). The maximum diameter of each patient's tumors was determined from the CT images. The tumor contours were subclassified as smooth or lobulated. The homogeneousness was assessed as homogeneous or heterogeneous on plain CT for three of the 56 TENs. On enhanced CT, the enhancement patterns were recorded as homogeneous or heterogeneous for the other 53 TENs.

Statistical analysis. Paired *t*-test statistics were used for the analysis between the T/M ratio1 and T/M ratio2 for each tumor type. To analyze the relationship between the tumor types and the T/M ratio, we employed the *t*-test for unpaired observations and a one-way analysis of variance (ANOVA) test followed by Bonferroni's multiple comparison test for more than 2 variables. We used receiver operating characteristic (ROC) curve analyses to determine the T/M ratio values for carcinoma in both the early and delayed scans that maximized the sensitivity and specificity.

For the CT features of the TENs, we used a multivariate logistic regression (MLR) analysis to estimate the probability (*p*-value), odds ratio (OR), and 95% confidence interval (CI) of the carcinomas. The analysis was first done in a univariate fashion, and then all of the covariates with a *p*-value < 0.10 in the univariate analysis were included in the multivariate analysis that yielded a model. We performed the ROC curve analysis to evaluate the predictive performance of the CT model by assessing its discrimination. Discrimination was assessed by the area under the curve (AUC).

All statistical analyses were performed using the SPSS Statistics 22 software program (IBM, Armonk, NY, USA). A *p*-value < 0.05 was considered significant for all analyses.

Results

Patients and tumor characteristics. A total of 56 patients met the criteria for the analysis of STP PET/CT scans. Forty-eight patients underwent surgical resection and the remaining eight patients underwent a core biopsy. Table 1 shows the characteristics of the patients. Histopathologically, 27 cases were classified as LR (9 type A, 7 type AB, and 11 type B1), 14 were classified as HR (9 type B2, 5 type B3), and 15 were classified as CA. The tumor long-axis diameter ranged from 15 to 107 mm with a mean of 53.04 mm in the LR cases, from 19 to 84 mm with a mean of 46.71 mm in the HR cases, and from 29 to 118 mm with a mean of 73.47 mm in the CA cases. A significant difference in diameter was identified between the HR and CA cases ($p = 0.010$) and between the LR and CA cases ($p = 0.022$). There was no significant difference in diameter between the LR and HR cases ($p = 0.449$).

A total of 35 patients met the criteria for the analysis of DTP PET/CT scans. Histopathologically, 17 cases were classified as LR (5 type A, 5 type AB, and 7 type B1), nine cases were classified as HR (7 type B2, 2 type B3), and nine cases were classified as CA. The tumor long-axis diameter ranged from 15 to 85 mm with a mean of 51.71 mm in the LR cases, from 19 to 84 mm with a mean of 43.44 mm in the HR cases, and from 32 to 100 mm with a mean of 71.50 mm in the CA cases. A significant difference in diameter was identified between the HR and CA cases ($p = 0.024$). There were no significant differences in diameter between the LR and HR cases ($p = 0.466$) or between the LR and CA cases ($p = 0.071$).

The tumor-to-mediastinum ratio on F-18 FDG PET/CT. In the STP scanning of all 56 patients, the mean T/M ratio 1 ± SD was 2.12 ± 0.762 (range, 0.77-4.34) for all of the TENs. In a simplified WHO classification scheme, the mean T/M ratio 1 ± SD was 2.18 ± 0.784 (range, 0.77-4.34) for the LR TENs, 2.00 ± 0.730 (range, 0.88-3.25) for the HR TENs, and 5.60 ± 5.68 (range, 1.31-24.6) for the CA TENs.

Table 2 shows the T/M ratio 1 and T/M ratio 2 values on the DTP scans for 35 patients. There were no significant differences between the T/M ratio 1 and T/M ratio 2 values for all 3 groups, *i.e.*, LR, HR, and CA. For all of these TENs, the mean T/M ratio 1 ± SD was 2.14 ± 0.818 (range, 0.77-4.34) and the T/M ratio 2 ± SD was 2.24 ± 0.955 (range, 0.86-4.76). In the simplified

Table 1 Characteristics of the patients and tumors

	Low-risk	High-risk	Carcinoma
No. of patients (%)	27 (48%)	14 (25%)	15 (27%)
Sex			
Male	16	6	10
Female	11	8	5
Age (mean yr, range)	59.00 (25–86)	64.93 (43–79)	59.53 (21–84)
Size (mm, range)	53.04 (15–107)†	46.71 (19–84)*	73.47 (29–118)
WHO classification			
A/AB/ B1	9/7/11		
B2/B3		10/4	
Carcinoma			15
Masaoka's classification			
Ⅰ	9	3	0
Ⅱ	12	7	1
Ⅲ	5	4	7
Ⅳa	0	0	3
Ⅳb	1	0	4

*$p = 0.010$ compared with thymic carcinoma.
†$p = 0.022$ compared with thymic carcinoma.

Table 2 Tumor/mediastinum ratios on dual-time-point (DTP) scans of 35 patients

WHO classification	No. of tumors	T/M ratio 1 (early)	T/M ratio 2 (delayed)
Low-risk group	17	2.20 ± 0.857	2.29 ± 0.984
Type A	5	2.44 ± 1.096	2.55 ± 1.307
Type AB	5	1.94 ± 1.053	2.03 ± 1.156
Type B1	7	2.20 ± 0.563	2.29 ± 0.664
High-risk group	9	2.02 ± 0.775	2.15 ± 0.949
Type B2	7	2.19 ± 0.742	2.37 ± 0.924
Type B3	2	1.44 ± 0.792	1.37 ± 0.721
Thymic carcinoma	9	3.57 ± 1.234	3.84 ± 1.558

T/M ratio = the ratio of the peak SUV of the tumor to the peak.
SUV of the aortic arch.
The data are mean ± SD.

WHO classification scheme, the mean T/M ratio ± SD was 2.20 ± 0.857 (range, 0.77-4.34) for T/M ratio 1 and 2.29 ± 0.984 (range, 0.97-4.76) for T/M ratio 2 in the LR TENs, 2.02 ± 0.775 (range, 0.88-3.25) for T/M ratio 1 and 2.15 ± 0.949 (range, 0.86-3.56) for T/M ratio 2 in the HR TENs, and 3.57 ± 1.234 (range, 1.31-5.24) for T/M ratio 1 and 3.84 ± 1.558 (range, 1.45-6.39) for T/M ratio 2 in the carcinomas. Nine of the 17 LR TENs, 5 of the nine HR TENs, and 6 of the 9 carcinomas showed a T/M ratio 2 that was higher than the T/M ratio 1.

The relationship between the tumor types and tracer uptake. In the STP scans of the 56 tumors, the T/M ratio 1 was significantly higher in the carcinomas than in all of the TENs ($p = 0.000276$). The T/M ratio 1 was significantly higher in the carcinomas than in both the LR TENs ($p = 0.002$) and the HR TENs ($p = 0.006$). No significant difference was identified in the T/M ratio 1 between the LR and HR TENs ($p = 1.000$)

As illustrated in Fig. 1 and 2, in the DTP scans of 35 of the tumors, the T/M ratio was significantly higher in the carcinomas than in all of the TENs on both the early and delayed scans ($p = 0.000388$ for T/M ratio 1; $p = 0.001$ for T/M ratio 2). The T/M ratio 1 was significantly higher in the carcinomas than in both the LR TENs ($p = 0.004$) and HR TENs ($p = 0.005$). No significant difference was identified in the T/M ratio 1 between the LR and HR TENs ($p = 1.000$). The T/M ratio 2 was significantly higher in the carcinomas than both in the

LR TENs ($p=0.008$) and HR TENs ($p=0.011$). No significant difference was identified in the T/M ratio 2 between the LR and HR TENs ($p=1.000$).

ROC curves and cut-off values for the T/M ratio. In the STP PET/CT for all 56 TENs, the ROC curve for T/M ratio 1 for predicting carcinoma revealed that the appropriate cut-off value for obtaining the highest accuracy was 2.39, with a sensitivity of 86.7%, specificity of 73.2%, and accuracy of 75.0%. The AUC of the STP scans was 0.855 (95% CI; 0.713-0.998, $p=0.000053$).

In the DTP PET/CT for the 35 TENs, the ROC curve for predicting carcinoma indicated that the appropriate cut-off value for the T/M ratio was 2.39 for T/M ratio 1, with a sensitivity of 88.9%, specificity of 73.1%, and accuracy of 74.3%, and 2.96 for T/M ratio 2, yielding a sensitivity of 88.9%, specificity of 80.8%, and accuracy of 82.9%. The AUC of the DTP scans was 0.838 (95% CI; 0.658-1.000, $p=0.03$) for the early scans and 0.825 (95% CI; 0.650-0.999, $p=0.004$) for the delayed scans (Table 3).

CT features associated with thymic carcinoma. The univariate analyses revealed that the tumors of the patients with carcinoma were significantly more likely to be larger ($p=0.009$), to include pleural effusion ($p=0.022$), to be homogeneous ($p=0.026$), and to be infiltrative to mediastinal fat ($p=0.001$) (Table 4). No significant differences were detected between the carcinomas and thymomas with respect to tumor contours,

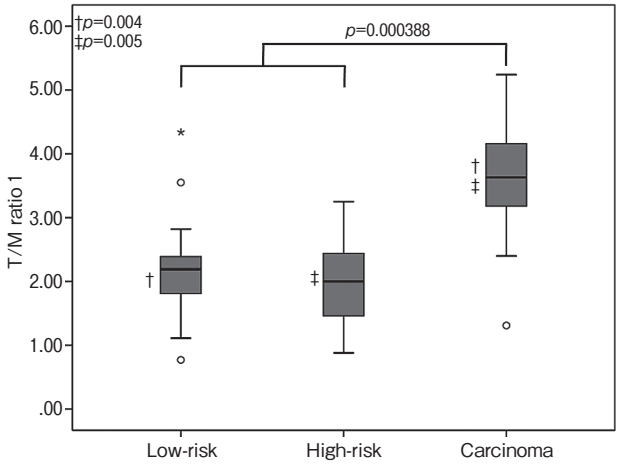

Fig. 1 The correlation between the tumor-to-mediastinum ratio on the 90-min early scans (the T/M ratio 1) and the simplified WHO classification scheme. The T/M ratio 1 was significantly higher in the thymic carcinomas than in all TENs ($p=0.000388$) and both the low-risk TENs ($p=0.004$) and high-risk TENs ($p=0.005$). No significant difference was identified between the low-risk and high-risk TENs ($p=1.000$).

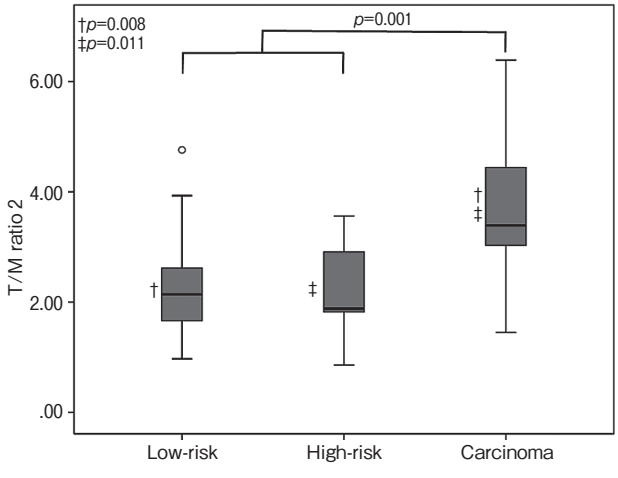

Fig. 2 The correlation between the tumor-to-mediastinum ratio on the 120-min delayed scans (the T/M ratio 2) and the simplified WHO classification scheme. The T/M ratio 2 was significantly higher in the thymic carcinomas than in all TENs ($p=0.001$) and both the low-risk ($p=0.008$) and high-risk TENs ($p=0.011$). No significant difference was identified between the low-risk and high-risk TENs ($p=1.000$).

Table 3 Diagnostic performance of each parameter for the prediction of thymic carcinoma

	No. of Patients	Threshold Value	Sensitivity (%)	Specificity (%)	Accuracy (%)	AUC
Single-time-point scan						
T/M ratio 1 (early)	56	2.39	86.7	73.2	75.0	0.855
Dual-time-point scan						
T/M ratio 1 (early)	35	2.39	88.9	73.1	74.3	0.838
T/M ratio 2 (delayed)	35	2.96	88.9	80.8	82.9	0.825
CT model						
Mediastinal fat infiltration	56	–	–	–	–	0.853

T/M ratio, the ratio of the peak standardized uptake value of the tumor to the peak standardized uptake value of aortic arch; CT, computed tomography; AUC, the area under the curve.

Table 4 Significant predictors of thymic carcinoma for all 56 patients

Variables	Thymic carcinoma	Thymoma	*P*-value	OR	95% CI
Tumor size (mm)	73.47	50.88	0.009	1.036	1.009–1.063
Pleural effusion			0.022	14.545	1.472–143.729
Positive	4	1			
Negative	11	40			
Homogeneousness			0.026	6.19	1.238–30.961
Homogeneous	2	20			
Heterogeneous	13	21			
Mediastinal fat invasion			0.001	17.727	3.435–91.496
Positive	13	11			
Negative	2	30			

Table 5 Multivariate logistic regression analysis for thymic carcinoma, 56 subjects

Variables	Regression coefficient	*P*-value	OR	95% CI
Mediastinal fat invasion	2.239	0.018	9.381	1.457–60.394
Pleural effusion	1.581	0.229	4.858	0.369–63.959
Homogeneousness	1.123	0.263	3.074	0.431–21.933
Size	0.002	0.934	1.002	0.965–1.039

the presence of calcification, great vessel invasion, or lymph node adenopathy. We entered the variables of tumor size, presence of pleural effusion, homogeneousness, and fat infiltration into the MLR analysis.

In the MLR analysis, mediastinal fat infiltration ($p=0.018$) was the predictor of carcinoma (Table 5). The ROC curve obtained for the CT model yielded an AUC of 0.853 (95% CI; 0.734-0.971, $p=0.000059$) (Fig. 3).

Discussion

The present study explored the correlation between the T/M ratio and the low-risk, high-risk and carcinoma groups of TEN cases on DTP PET/CT and the diagnostic capacity of PET/CT scans with ROC analyses. With either early or delayed scans for discriminating carcinoma from thymoma, our ROC analyses showed acceptable diagnostic accuracy. In addition, the MLR analysis demonstrated that mediastinal fat infiltration was a predictor that had moderate accuracy. These results show that the measurement of T/M ratio and the observation of CT features are important predictors of carcinoma and that, with the use of an ROC analysis, there is no distinction between the capabilities for diagnosis of carcinoma of one modality from that of the other.

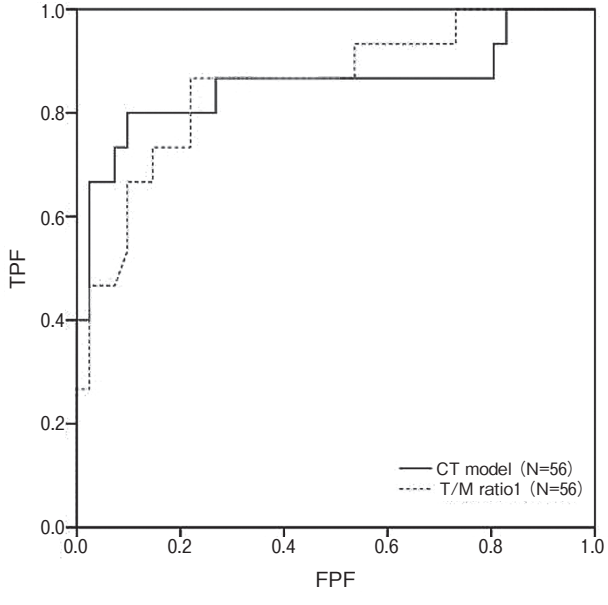

Fig. 3 ROC curve for the thymic carcinomas. The AUC value derived from the tumor-to-mediastinum ratio on the 90-min early scan (T/M ratio1) was 0.855 (95% CI 0.713–0.998, $p=0.000053$). The AUC derived from the multivariate logistic CT model was 0.853 (95% CI 0.734–0.971, $p=0.000059$).

Several clinical PET studies demonstrated the usefulness of STP PET for evaluations of the malignant nature of TEN and the correlation between FDG uptake

and the WHO classification [7-13]. Previous investigations showed that STP PET has an accuracy of 79-88.5% for the detection of carcinomas [9, 11-13]. Inoue *et al.* first mentioned delayed scanning for thymic tumors, and they observed that 3-h delayed SUVmax values were higher than the early SUVmax values in all but 2 of 23 thymomas and three carcinomas [11]. However, they could find no advantages of 3-h delayed scanning for differentiating tumors.

In the present study, the AUC values were in the same range with moderate accuracy (0.838 for T/M ratio 1; 0.825 for T/M ratio 2). Using the cut-off values, the present study yields an accuracy of 82.9% for the delayed scanning, which is higher than the accuracy of 74.3% for the early scanning in 26 thymomas and nine thymic carcinomas. We hypothesize that the 2-h delayed scans may have the potential to slightly improve the diagnostic capacity of PET/CT for the diagnosis of carcinoma compared with that for the 90-min early scans. The reason for the difference between the previous [11] and present studies may be a difference in study design, such as the evaluation method (SUVmax or T/M ratio), or the scan time-points for the DTP scans. The clinical significance of DTP scanning thus remains a controversial issue, and a prospective study with a larger number of patients is still needed to determine the diagnostic capacity of DTP scans in patients with TENs.

An earlier report mentioned that CT findings of irregular contour, necrotic or cystic component, heterogeneous enhancement, lymphadenopathy, and great vessel invasion were more commonly seen in carcinomas than low- or high-risk thymomas [20]. The present study's MLR analysis and ROC analysis demonstrated that fat infiltration is a predictor of thymic carcinoma with moderate accuracy. These discrepancies between studies may be due to (1) the relatively small number of patients and/or (2) the differing proportions of the WHO classification and/or clinical-pathologic stage.

In contrast, Jeong *et al.* found that three features, *i.e.*, lobulated contour, mediastinal fat invasion, and great vessel invasion were all more often seen in carcinomas than low-risk thymomas [6], and Sung *et al.* demonstrated by a discriminant analysis that mediastinal fat invasion on enhanced CT was an indicator for differentiating 3 risk groups in 33 TENs, with a prediction rate of approx. 76% [7]. These results suggest that the finding of mediastinal fat infiltration has the potential to improve the diagnostic accuracy for carcinoma.

However, at this time the CT findings are not sufficient to change the standard criteria for open biopsy based on CT morphology. The number of patients included in our study was too small to draw conclusions, but our data suggest that the CT finding of mediastinal fat invasion may have the potential to serve as a preoperative predictor of carcinoma with moderate diagnostic capacity.

Our study is limited by the relatively small number of patients included and the retrospective design. Further prospective investigations using a larger patient population comparing PET/CT and chest CT would be useful for evaluating the role of a DTP PET/CT scan and a chest CT for predicting carcinoma. Despite its limitations, this study was the first to evaluate the diagnostic capacity of DTP scans for TEN using ROC analyses. Moreover, our study included a direct comparison between PET/CT and chest CT with regard to diagnostic efficacy for the discrimination of carcinoma from thymoma.

In conclusion, the findings of the present study provide further evidence that PET/CT is an important noninvasive method for the evaluation of TEN using the T/M ratio. Two-hour delayed scanning could have the potential to improve the diagnostic capacity for the diagnosis of carcinoma. Measurements of the T/M ratio and the detection of mediastinal fat infiltration are important predictors of carcinoma, and they could be predictive of carcinoma with moderate diagnostic accuracy. Moreover, each of these imaging parameters could be useful tools to avoid making the wrong diagnosis and to improve the reliability of those 2 modalities. We also observed no distinction between the capabilities of one modality from that of the other for the diagnosis of carcinoma.

References

1. Travis WD, Brambilla E, Muller-Hermelink HK and Harris CC: Pathology and genetics of tumors of the lung, pleura, thymus and heart; in WHO Classification of Tumors, Kleihues P, Sobin LH eds, 2nd Ed, IARC Press, Lyon (2004) pp145−197.
2. Detterbeck FC: Clinical value of the WHO classification system of thymoma. Ann Thorac Surg (2006) 81: 2328−2334.
3. Kondo K: Tumor-node metastasis staging system for thymic epithelial tumors. J Thorac Oncol (2010) 5: 352−356.
4. Chen G, Marx A, Chen WH, Yong J, Puppe B, Stroebel P and Mueller-Hermelink HK: New WHO histological classification predicts prognosis of thymic epithelial tumors: a clinicopathologic

study of 200 thymoma cases from China. Cancer (2002) 95: 420–429.
5. Marchevsky AM, Gupta R, McKenna RJ, Wick M, Moran C, Zakowski MF and Suster S: Evidence-based pathology and the pathologic evaluation of thymomas: the World Health Organization classification can be simplified into only 3 categories other than thymic carcinoma. Cancer (2008) 112: 2780–2788.
6. Jeong YJ, Lee KS, Kim J, Shim YM, Han J and Kwon OJ: Does CT of thymic epithelial tumors enable us to differentiate histologic subtypes and predict prognosis? AJR Am J Roentgenol (2004) 183: 283–289.
7. Sung YM, Lee KS, Kim BT, Choi JY, Shim YM and Yi CA: 18F-FDG PET/CT of thymic epithelial tumors: usefulness for distinguishing and staging tumor subgroups. J Nucl Med (2006) 47: 1628–1634.
8. Endo M, Nakagawa K, Ohde Y, Okumura T, Kondo H, Igawa S, Nakamura Y, Tsuya A, Murakami H, Takahashi T, Yamamoto N, Ito I and Kameya T: Utility of 18FDG-PET for differentiationg the grade of malignancy in thymic epithelial tumors. Lung Cancer (2008) 61: 350–355.
9. Shibata H, Nomori H, Uno K, Sakaguchi K, Nakashima R, Iyama K, Tomiyoshi K, Kaji M, Goya T, Suzuki T and Horio H: ^{18}F-fluorodeoxyglucose and ^{11}C-acetate positron emission tomography are useful modalities for diagnosing the histologic type of thymoma. Cancer (2009) 115: 2531–2538.
10. Fukumoto K, Taniguchi T, Ishikawa Y, Kawaguchi K, Fukui T, Kato K, Matsuo K and Yokoi K: The utility of [18F]-fluorodeoxyglucose positron emission tomography-computed tomography in thymic epithelial tumours. Eur J Cardiothorac Surg (2012) 42: 152–156.
11. Inoue A, Tomiyama N, Tatsumi M, Ikeda N, Okumura M, Shiono H, Inoue M, Higuchi I, Aozasa K, Johkoh T, Nakamura H and Hatazawa J: (18)F-FDG PET for the evaluation of thymic epithelial tumors: Correlation with the World Health Organization classification in addition to dual-time-point imaging. Eur J Nucl Med Mol Imaging (2009) 36: 1219–1225.
12. Sasaki M, Kuwabara Y, Ichiya Y, Akashi Y, Yoshida T, Nakagawa M, Murayama S and Masuda K: Differential diagnosis of thymic tumors using a combination of 11C-mehionine PET and FDG PET. J Nucl Med (1999) 40: 1595–1601.
13. Toba H, Kondo K, Sadohara Y, Ostuka H, Morimoto M, Kajiura K, Nakagawa Y, Yoshida M, Kawakami Y, Takizawa H, Kenzaki K, Sakiyama S, Bando Y and Tangoku A: 18F-fluorodeoxyglucose positron emission tomography/computed tomography and the relationship between fluorodeoxyglucose uptake and the expression of hypoxia-inducible factor-1α, glucose transporter-1 and vascular endothelial growth factor in thymic epithelial tumours. Eur J Cardiothorac Surg (2013) 44: 105–112.
14. Shinya T, Rai K, Okumura Y, Fujiwara K, Matsuo K, Yonei T, Sato T, Watanabe K, Kawai H, Sato S and Kanazawa S: Dual-time-point F-18 FDG PET/CT for evaluation of intrathoracic lymph nodes in patients with non-small cell lung cancer. Clin Nucl Med (2009) 34: 216–221.
15. Shinya T, Fujii S, Asakura S, Taniguchi T, Yoshio K, Alafate A, Sato S, Yoshino T and Kanazawa S: Dual-time-point F-18 FDG PET/CT for evaluation in patients with malignant lymphoma. Ann Nucl Med (2012) 26: 616–621.
16. Suga K, Kawakami Y, Hiyama A, Sugi K, Okabe K, Matsumoto T, Ueda K, Tanaka N and Matsunaga N: Differential diagnosis between (18)F-FDG-avid metastatic lymph nodes in non-small cell lung cancer and benign nodes on dual-time point PET/CT scan. Ann Nucl Med (2009) 23: 523–531.
17. Masaoka A, Monden Y, Nakahara K and Tanioka T: Follow-up study of thymomas with special reference to their clinical stages. Cancer (1981) 48: 2485–2492.
18. Terzi A, Bertolaccini L, Rizzardi G, Luzzi L, Bianchi A, Campione A, Comino A and Biggi A: Usefulness of 18-F FDG PET/CT in the pre-treatment evaluation of thymic epithelial neoplasms. Lung Cancer (2011) 74: 239–243.
19. Viti A, Bertolaccini L, Cavallo A, Fortunato M, Bianchi A and Terzi A: 18-Fluorine fluorodeoxyglucose positron emission tomography in the pretreatment evaluation of thymic epithelial neoplasms: a metabolic biopsy confirmed by Ki-67 expression. Eur J Cardiothorac Surg (2014) 46: 369–374.
20. Sadohara J, Fujimoto K, Müller NL, Kato S, Takamori S, Ohkuma K, Terasaki H and Hayabuchi N: Thymic epithelial tumors: comparison of CT and MRI imaging findings or low-risk thymomas, high-risk thymomas, and thymic carcinomas. Eur J Radiol (2006) 60: 70–79.